

Journal of Materials Chemistry C

Accepted Manuscript



This is an *Accepted Manuscript*, which has been through the Royal Society of Chemistry peer review process and has been accepted for publication.

Accepted Manuscripts are published online shortly after acceptance, before technical editing, formatting and proof reading. Using this free service, authors can make their results available to the community, in citable form, before we publish the edited article. We will replace this *Accepted Manuscript* with the edited and formatted *Advance Article* as soon as it is available.

You can find more information about *Accepted Manuscripts* in the [Information for Authors](#).

Please note that technical editing may introduce minor changes to the text and/or graphics, which may alter content. The journal's standard [Terms & Conditions](#) and the [Ethical guidelines](#) still apply. In no event shall the Royal Society of Chemistry be held responsible for any errors or omissions in this *Accepted Manuscript* or any consequences arising from the use of any information it contains.



Journal Name

ARTICLE

Tunable RGB luminescence of single molecule with high quantum yields through a rational design

Wen Li,^a Yu-Mo Zhang,^{*b} Ting Zhang,^a Weiran Zhang,^a Minjie Li,^{*a} and Sean Xiao-An Zhang^{*a}

Received 00th January 20xx,
Accepted 00th January 20xx

DOI: 10.1039/x0xx00000x

www.rsc.org/

Organic smart materials with Red, Green, and Blue emissions are important in fabricating full-color display device, multi-functional sensor, etc. However, achieving RGB emission with high quantum yields using a single-molecule material has proved challenging. In this paper, a new stimuli responsive RGB luminescent organic molecule RHBT-G with high quantum yields was rationally designed based on the combination of an AIEE luminophore and a fluorescent molecular switch. The ESIPT and TBET mechanism were introduced to realize the RGB emission with single 365nm excitation light in solution and PMMA film. X-ray single crystal diffraction, UV-Vis and photoluminescence(PL) spectra are carried out to prove the working mechanism of the dye. The rational design will accelerate the development of stimuli-responsive materials with excellent optical properties.

Introduction

Smart luminescent organic materials responsive to environment stimuli reversibly have gain great interests for their potential applications in display¹, security inks², sensors³, etc. Exploring smart luminescent materials with red (R), green (G) and blue (B) emission is of great importance for full-color display device, multi-functional sensor. Compared to mixing several materials emitting different lights, RGB luminescence of a single organic molecule is still less reported. Successful examples realizing RGB emission of single molecule generally adopted the following two strategies: The first one is mixing different luminophores into one molecule to form a complex energy transfer system or mixing different forms of the molecule in the solution⁴. The other one is changing the π -conjugation of the molecules which contain only one π -conjugated luminophore by altering the conformation or stacking array under different conditions⁵. Compared to the second strategy, the first one is more directional and renders the molecules or systems with relatively predictable emissions. However, inconvenience do exist such as different excitation light must be used and low quantum yield of certain emission may occur. To address the challenges, we decided to present a novel design based on the first strategy.

In order to realize the RGB emission with the single 365 nm excitation light which is most commonly used and commercially available, the interference of each chromophore (red, green and blue) should be narrowed to the minimum. As

a stimuli-responsive molecule, each luminophore would be better to work independently towards different stimuli which could diminish the interference to some degree if different forms of the molecule could be transformed completely. But attention must be paid to the pattern of linkage of each chromophore to prevent the change of the conjugation of each chromophore which might influence the original emissions of them. Moreover, to get a strong intensity of the green and red emission with a large Stokes shift excited with 365 nm light, some special mechanisms such as excited state intramolecular proton transfer (ESIPT)⁶ and energy transfer must be introduced to realize the large Stokes shift.

Herein, we report a rational design based on the combination of an AIEE luminophore with ESIPT properties and an acid-responsive fluorescent molecular switch to realize RGB emission with high quantum yields in solution and PMMA film.

Results and discussion

Molecule design and synthesis

RHBT-G was designed and synthesized as shown in Supporting Information. The benzamide of 2-(2-hydroxyphenyl)-benzothiazole (HBT) was reported to be an aggregation induced emission enhanced (AIEE) luminophore emitting green light with high quantum yield in the aggregates which possesses ESIPT property.⁷ The phenolic hydroxyl group is sensitive to base and a blue emission is expected when the molecule is stimulated with base. The xanthene moiety of rhodamine B possessing switchability thanks to the spiro- γ -lactam structure which could be turned on by acid works as the red luminophore with a high quantum yield in dilute solution. What's more, the phenyl ring with a large torsion an-

a. State Key Laboratory of Supramolecular Structure and Materials, College of Chemistry, Jilin University, Changchun, Jilin 130012, China. E-mail: liminjie@jlu.edu.cn; seanzhang@jlu.edu.cn.

b. College of Chemistry, Jilin University, Changchun, Jilin 130012, China. E-mail: zhangyumo@jlu.edu.cn. Fax: +86-431-85163812; Tel: +86-431-85163810

† Electronic supplementary information (ESI) available. See DOI:10.1039/x0xx00000x

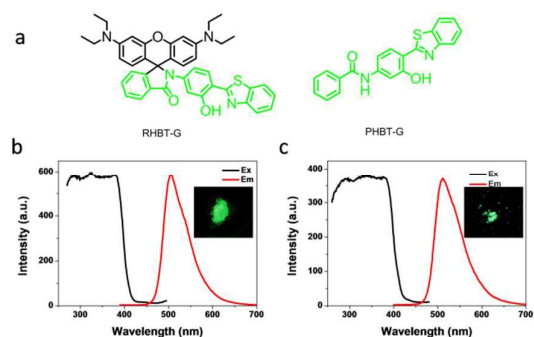


Fig.1 (a) Molecular structures of **RHBT-G** and **PHBT-G**; (b) Photoluminescence (PL) spectra of **RHBT-G** powders. Inset: Photograph of the powder under portable 365nm light. (c) PL spectra of **PHBT-G** powders. Inset: Photograph of the powder under portable 365nm light.

gle to the xanthene moiety could work as a rigid conjugated spacer preventing the conjugation of the two luminophores and offering the molecule with the possibility of through bond energy transfer (TBET).⁸ The reason why we select an AIEE luminophore is that the low quantum yield in solution of the green emission contributes little to the mixed emission guaranteeing the purity of the emission when the other luminophore with much higher quantum yield emits in case the molecule couldn't be transformed completely. **RHBT-G** and the reference molecule **PHBT-G** were simply synthesized in four steps with moderate yields. All the compounds were fully characterized with ¹H NMR, ¹³C NMR, and mass spectroscopy (Fig.S32-S39, ESI⁺).

Solid optical properties and X-ray and crystallography

RHBT-G exhibited vivid green luminescence excited with 380nm in the solid state with high absolute quantum yield (ϕ_r) (Fig. 1). Actually, the solid luminescent behaviour of **RHBT-G** ($\lambda_{em}=510\text{nm}$, $\phi_r=57\%$) with a large Stokes shift due to ESIPT was inherited from **PHBT-G** ($\lambda_{em}=505\text{nm}$, $\phi_r=41\%$) perfectly. The xanthene moiety of **RHBT-G** has little effect on the band gap of the bottom luminophore but has a positive effect on the quantum yield.

To gain deeper understanding of the solid emission of **RHBT-G**, the data of the single crystal which was obtained from slow diffusion of the good solvent CH_2Cl_2 into the poor solvent MeOH was analysed. Seen from the crystals of **RHBT-G** (Fig.2), the HBT moiety was almost coplanar due to the intramolecular hydrogen bond and only a partial overlap of the thiazole moiety between the adjacent molecules existed with a perpendicular distance about 3.766 Å suggesting a relatively weak π - π interaction which was a positive factor to maintain high quantum yield in the solid state. The xanthene moiety of the neighbouring molecule was almost perpendicular to the benzothiazole moiety with a C-H $\cdots\pi$ interaction which was in favour of the rigidity of the crystal, probably leading to a higher quantum yield than **PHBT-G**.

AIEE property and TD-DFT calculations

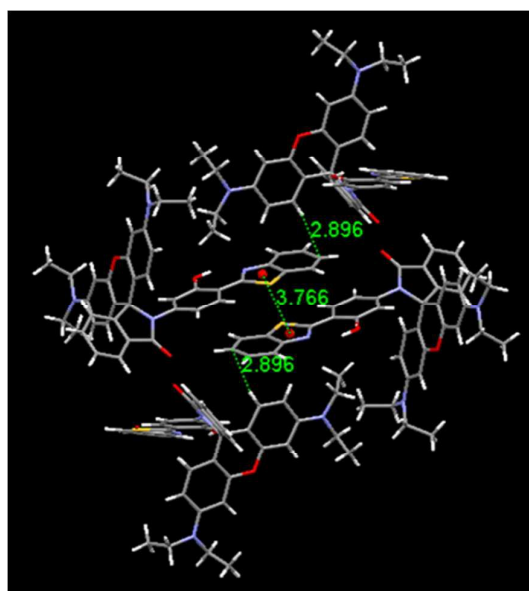


Fig.2 Crystal structure of **RHBT-G**.

The THF solution of **RHBT-G** was scarcely emissive with the relative quantum yield (ϕ_{ref}) in relative to anthracene measured to be 1% (Fig.S30, ESI⁺) which suggested the AIEE property was also inherited. So the emission behaviour of **RHBT-G** in THF and THF/water mixtures with varying water fractions was monitored. From the absorption spectra of **RHBT-G** in Fig.3a, when the water fraction was more than 80%, a slight red shift of the peak between 350nm and 400nm which was ascribed to the **PHBT** moiety according to the absorption spectra in Fig.S13 and the literature⁷ occurred suggesting the J-aggregation started to form. The slight blue shift and decrease of the peak when the water fraction was between 60-70% may be caused by the result of the interruption of the intramolecular hydrogen bond by water leading to the destruction of the coplanarity and a decreased conjugation of the **HBT** chromophore. Accordingly, the PL spectra in Fig.3b showed a drastic increase of the intensity when the water fraction reached 80% and a continuous increase following the increase of water until 95% ($\lambda_{em}=515\text{nm}$, $\phi_r=19\%$). The decrease of the intensity at 99% might be caused by the formation of larger nanoparticles with smaller specific surface area. The PL spectra also demonstrated a slight red shift of 5-8 nm between the free molecule in pure THF and the aggregates in 80% water as shown in Fig. S1. The J-aggregation was in accordance with the results of the TD-DFT calculations⁹ based on the single crystal data. Since the disordered structure of benzothiazole caused by the free rotation of the single bond of the aniline, two different circumstances were considered and in both situation the angle between the transition dipole and interconnected axis was lower than 54.7°. (Fig S2-S3, ESI⁺)¹⁰ The typical J-aggregation was considered in favour of the solid emission of **RHBT-G**.¹¹ The transition dipole was calculated using the dipole moment with the largest oscillation strength of which the corresponding molecular orbitals (HOMO-2 and LUMO) were

mainly distributed on the PHBT moiety rather than xanthene moiety as shown in Fig.S4-S7.

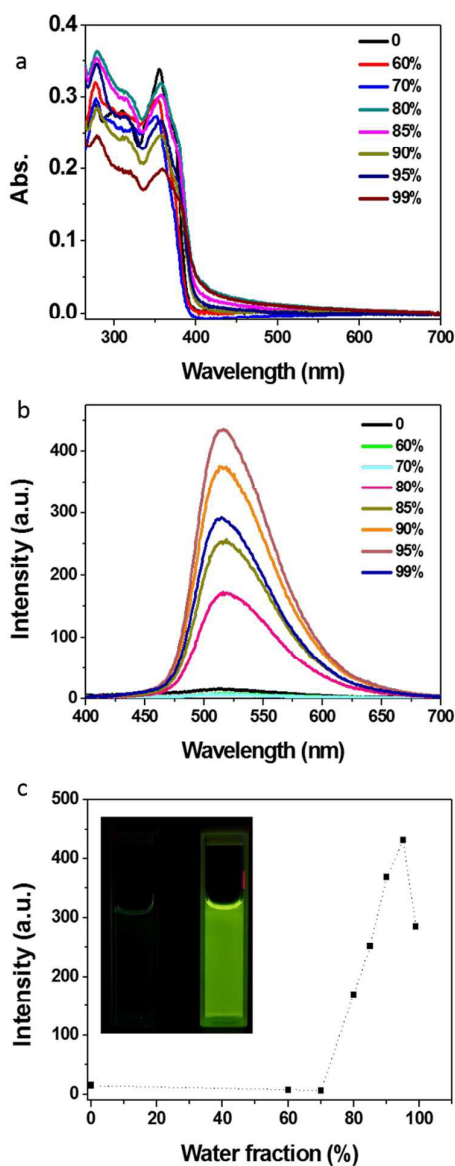


Fig.3 (a) UV-Vis and (b) PL spectra of 1.0×10^{-5} M **RHBT-G** in the THF/water mixture with different water fraction. (c) Changes of the PL intensity at 520 nm with different water fraction. Inset: photograph of the solution with water fraction of 0 and 95%

Optical properties in response to acid

To realize the red emission of **RHBT-G**, the optical behaviours under different concentration of TFA in THF were monitored. As shown Fig.S8, a new peak at 557nm characterized of the ring-opening form of the xanthene moiety emerged and continuously increased as the concentration of TFA increased. The solution turned pink from colourless with vivid orange-red emission ($\lambda_{em}=580\text{nm}$, $\phi_{ref}=44\%$). Unlike the continuous increase of the absorption spectra, the intensity of the fluorescence spectra excited with 557nm reached to the

maximum with 0.2 M TFA and stayed almost unchanged between 0.2 M and 0.5 M TFA as shown in Fig S9. The quenching effect of the proton solvent and the aggregation caused quenching (ACQ) effect are the common factors to influence Rhodamine dyes and were probably attributed to the unchanged intensity of the fluorescence. As we expected, the AIEE-active green emission of the still closed **RHBT-G** wasn't detectable or visible with 0.2 M TFA using the 365 nm excitation light (Fig.4) proving the necessity of choosing an AIEE luminophore to avoid a mixed emission. From the excitation spectra (Fig.S10, ESI⁺), a small peak between 330nm and 370nm existed and was higher than that of Rhodamine B. When excited with 365 nm light, **RHBT-G** showed a three times stronger red emission than Rhodamine B although the intensity of Rhodamine B excited with 545nm was much stronger than that of **RHBT-G**. Since the bottom green luminophore was an AIEE motif with weak emission in solution due to the non-radiative transition caused by vibration and rotation, Förster resonance energy transfer (FRET) was probably not the main attribute for this phenomenon. However, TBET was reported to be 2 orders faster than the through space energy transfer of the Förster model which could neglect the vibration and rotation to some extent¹² and was considered to be the cause for this large pseudo-Stokes shift. Of course, the response towards acid was reversible proved by the absorption and fluorescence spectra (Fig.S11, ESI⁺). When the same equivalent of triethylamine (TEA) was added to neutralize the acid, the spectra recovered indicating no side reaction occurred in this process.

During our further investigation of the effect of TFA, we surprisingly found that **RHBT-G** in the mix solution of THF and TFA with the volume ratio of 3:7 emitted a strong blue light ($\lambda_{em}=430\text{nm}$, $\phi_{ref}=41\%$) with the solution becoming colourless. (Fig. S12, ESI⁺) In order to get a deeper understanding of this phenomenon, the absorption and fluorescence spectra of **PHBT-G** under different conditions were obtained (Fig.S13-S14, ESI⁺). As shown in Fig.S13, **RHBT-G** exhibited a similar absorption peak with **PHBT-G** mainly cov-

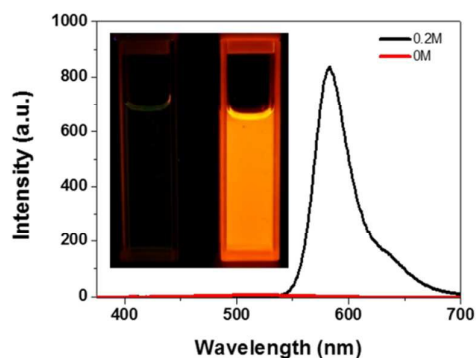


Fig.4 PL spectra of 1.0×10^{-5} M **RHBT-G** in THF with 0 M and 0.2 M TFA excited with 365 nm light. Inset: Photograph of the solution with 0 M and 0.2 M TFA under hand-held 365nm light.

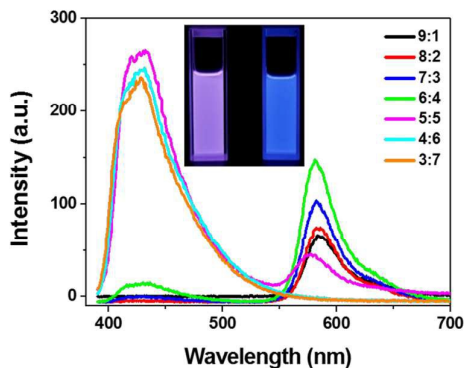


Fig.5 PL spectra of 1.0×10^{-5} M **RHBT-G** in the THF/TFA mixture with different volume ratio. Inset: photograph of the mixture with the THF/TFA volume ratio of 5:5 and 4:6.

erring between 300nm and 380nm. The peak shifted to the range between 390nm and 420nm due to the protonation of thiazole when acid exceeded the THF/TFA volume ratio of 4:6. Correspondingly, the fluorescence spectra in Fig.S14 showed the same blue emission centred at 430nm of the two compounds when TFA was more than the volume ratio of 4:6. The results undoubtedly proved that the blue emission originated from the protonation of **PHBT-G**. The disappearing of the peak in the visible region of the xanthen moiety was most probably due to further protonation of xanthen turning the donor-acceptor pairs into the acceptor-acceptor pairs leading to the interruption of the ICT process of the xanthen moiety. More detailed proofs could be gained when analysing the whole protonation process. As shown in the absorption spectra of Fig.S12, with the volume ratio of THF/TFA changing from 9:1 to 6:4 the peak centred between 300 and 350nm gradually decreased and the peak at 400nm attributed to the protonation form of **PHBT-G** moiety gradually increased and reached to the max at the volume ratio of 6:4. This process belonged to forming the divalent cation due to the protonation of thiazole moiety from the ring-opening monovalent cation of **RHBT-G** and a mixture of the two forms coexisted during the process. With further increasing TFA to the ratio of 5:5, the peak at 557nm decreased dramatically, indicating the formation of the trivalent cation due to further protonation on the xanthen moiety. The peak between 300nm and 350nm decreased to the lowest suggesting the completion of the protonation on the thiazole moiety, so the divalent and trivalent forms coexisted in the solution. As the TFA increased to the ratio of 7:3, the trivalent cation predominated with the red colour disappearing completely and the peak at 400nm lowered and narrowed to form the new peak at 370nm. Interestingly, the dominant divalent cation didn't show strong blue emission at the volume ratio of 6:4, but suddenly increased at the ratio of 5:5 when xanthen moiety was largely protonated with the purple emission shown in Fig.5. That is to say, **TBET** still existed in the divalent cation and only when the xanthen moiety was further protonated, the blue emission could be seen. From Fig.S13-S14, the truth could be gained that **PHBT-G** was scarcely protonated when

less than 0.9 M TFA was added indicating only the neutral and monovalent forms of **RHBT-G** existed in the condition of Fig.4. It could be further proved by that the absorption peak belonged to **PHBT-G** moiety stayed unchanged before 0.7 M TFA was added. So the acid effect could be concluded as shown in Scheme S2, ESI⁺. We also tried to prove the process by monitoring ¹H NMR under different conditions in CD₂Cl₂. Comparing Fig. S16 to Fig. S15, we can see when 0.05 mlCF₃COOD was added, the triplet peak belonging to “-CH₃” of N, N-diethylamino group split into two triplet peaks, and peak of the “-CH₂-” became a quintet peak from the original quartet peak. All the aromatic hydrogens became more complex and the integral was no longer close to an integer. All these characteristics proved that mixed forms exist under this condition. Since the chemical shift of all the hydrogens changed a lot and were totally different to the neutral form, the monovalent and divalent cations were deduced to coexist now. From Fig. S17, the peaks of aromatic hydrogens became simple again and the integrals were close to integers meaning a single form existing when 0.1 mlCF₃COOD was added. The quartet peak of “-CH₂-” turned into two broad peaks with equal integral which was an evident proof of the protonation of the N, N-diethylamino group on the xanthen which caused different chemical environment of the “-CH₂-” linked to the different nitrogen atom. And all the aromatic hydrogens shifted irregularly a lot compared to Fig.S10 which was not possibly caused by the change of the solvents, so the nitrogen of the thiazole was believed to protonated as well so the trivalent cation was obtained and proved under this condition. All the changes and trends could be seen clearly from fig. S18 and S19. Overall, the UV-Vis spectra, PL spectra of **RHBT-G** and the reference molecule **PHBT-G**, the NMR spectra all support our hypothesis very well.

Optical properties in response to base

The response to base of **RHBT-G** was investigated to realize a different emission. As shown in Fig.S20, a new peak centred at 396nm characterized of phenol oxygen anion emerged with the addition of base. As shown in Fig.6, the peak centred at 520 nm excited with 355nm of the neutral form decreased, while a new peak located at 460nm excited with 400nm of the anion form with a small Stokes shift increased. The max intensity of the blue emission was only a little higher than the green emission which meant the quantum yield of the anionic luminophore was not high enough and still quite suffered from the non-radiative decay. The small emission peak located at 400nm was considered to be the normal emission of **RHBT-G** without ESIPT because of the breakage of intramolecular hydrogen bond by the introduction of methanol, a kind of protic solvent. Of course, the response behaviour was also reversible seen from the spectra of Fig.S21.

Optical properties and responsive behavior of the PMMA film

In order to make the RGB luminescent molecule **RHBT-G**

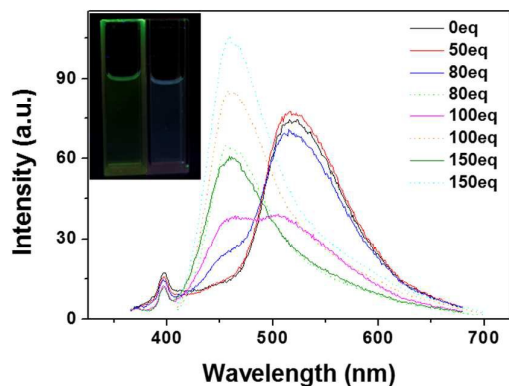


Fig.6 PL spectra of 1.0×10^{-5} M RHBT-G in the THF/Methanol (volume ratio:80/20) mixture with different amounts of sodium methoxide. (Solid line:excited with 355nm, dash line: excited with 400nm)

more convenient for application, the PMMA film of 1% wt. RHBT-G was made. 20% wt. propylene carbonate was doped as the plasticizer to prevent the compactness of PMMA and enhance the responding rate. All the ingredients were dissolved with dichloromethane and a trace of TEA to neutralize the acid generated by CH_2Cl_2 . The as-prepared film showed strong green emission ($\lambda_{\text{em}}=505\text{nm}$, $\phi_{\text{f}}=31\%$) under hand-held 365nm light. To our delight, the film treated with diethylamine (DEA) emitted strongly ($\lambda_{\text{em}}=450\text{nm}$, $\phi_{\text{f}}=30\%$) declaring that the rigid environment could restrict the rotation and vibration of the anion form which was proved by the PL spectra in Fig.S23 by changing the viscosity of the solution by adding glycerol. The intensity at 450 nm gradually increased as the volume ratio of glycerol increase from 60% to 90% proving the viscosity-dependent nature of the luminophore. The blue emission of the film could be recovered by heating under 70°C for 5 minutes. The film also exhibited a fast response towards the acidic vapor and a similar luminescent behavior compared to the solution. Fumed with the vapor of TFA for several seconds, the film emitted blue light strongly ($\lambda_{\text{em}}=430\text{nm}$, $\phi_{\text{f}}=33\%$) without any color to the naked eye which was the same with the emission peak in solution of the trivalent cation (Fig.S22, ESI⁺). The blue emission was not stable and turned to red emission ($\lambda_{\text{em}}=595\text{nm}$, $\phi_{\text{f}}=84\%$, ex: 365nm) within one minute at 70°C with a little red shift compared to the solution due to the aggregation to some degree. And, the red emission was stable and can be recovered only by fuming with base. Owing to the ESIPT and TBET mechanism, besides the blue emission, both the green and red emission of the film could emit brightly excited with the commonly used 365 nm light. The working mechanism was concluded as shown in Fig.7. To further prove the working mechanism, TD-DFT calculation had been carried out using B3LYP/6-31+g (d) method. As shown in Fig.S24, the allowed transition with max probability was from HOMO-2 to LUMO both of which distributed on benzothiazole, proving the PHBT moiety was the luminophore in the neutral form. The ground state of the monovalent cation in Fig. S25 showed two transition ways on the xanthene and PHBT moiety-

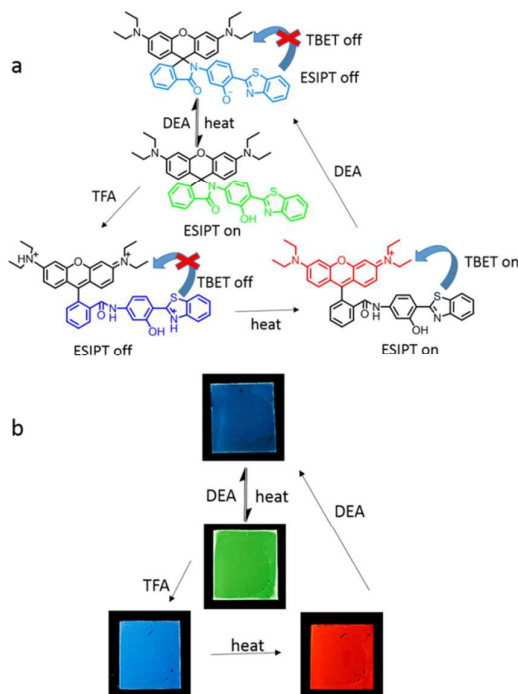


Fig.7 (a) Transformation and mechanism of the tunable RGB luminescence excited with 365nm light.(b)Photographs of the RGB luminescence in PMMA film.

ies respectively, however, the excited state in Fig.S26 showed only one radiative transition from the xanthene moiety without the fluorescence of PHBT moiety. These results clearly proved the TBET process existing in the monovalent cation in a theoretical way. And the rest HOMOs and LUMOs of the allowed transitions with largest probabilities in Fig.S27-29 all distributed on the luminophores in accordance with our assumptions.

As a concept of proof, we tried to find some applications in anti-counterfeiting and information storage using the PMMA solution. By writing on a glass using a plastic dropper filled with the PMMA film, the letters could emit strongly after several seconds for drying the CH_2Cl_2 . After treating the letters with DEA, TFA, and heating, the information emitting RGB light could be recorded easily as shown in Fig 8a. Potential applications in anti-counterfeiting was also demonstrated by writing a green "5" on the "money". Only when the "5" emitted blue after treated with base and emitted red after treated with acid and heated, can the "money" possibly be genuine as shown in Fig 8.

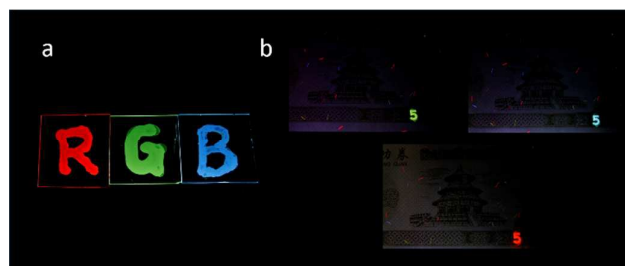


Fig.8 (a) Photograph of a simple Information storage device with the letters

emitting different lights. (b) Photographs of the “money” with our molecules written on it as a way of anti-counterfeiting.

Conclusions

In summary, we have designed and synthesized RHBT-G composed of an AIEE luminophore and fluorescent switch that is responsive to the acid/base to realize the RGB emission with single molecule both in solution and PMMA film. Due to the ESIPT and TBET mechanisms, all the emission could be realized excited with 365nm light with high quantum yields. The multichannel of the distinctive optical signal endows RHBT-G with potential applications in anti-counterfeiting and logic gates with prominent colour contrast of the luminescence. And we believe the ration design will be suitable for designing more smart materials with excellent sensitivity and optic properties.

Acknowledgements

This work was supported by the National Science Foundation of China (Grant No.51373068, No.51303063) and the program of Chang Jiang Scholars and Innovative Research Team in University (IRT101713018) for financial support.

Notes and references

- D. Li, H. Zhang, C. Wang, S. Huang, J. Guo and Y. Wang, *J. Mater. Chem.*, 2012, **22**, 4319; Y.M. Zhang, W. Li, X. Wang, B. Yang, M. Li and S. X. A. Zhang, *Chem. Commun.*, 2014, **50**, 1420-1422; Y. M. Zhang, X. Wang, W. Zhang, W. Li, X. Fang, B. Yang, M. Li and S. X. A. Zhang, *Light: Science & Application*, 2015, **4**, e249.
- Q. Qi, Y. f. Liu, X. Fang, Y. Zhang, P. Chen, Y. Wang, B. Yang, B. Xu, W. Tian and S. X. A. Zhang, *RSC Adv.*, 2013, **3**, 7996–8002; Y. Deng, D. Zhao, X. Chen, F. Wang, H. Song and D. Shen, *Chem. Commun.*, 2013, **49**, 5751–5753; W. Lin, Q. Zhao, H. Sun, K. Y. Zhang, H. Yang, Q. Yu., X. Zhou, S. Guo, S. Liu and W. Huang, *Advanced Optical Materials*, 2015, **3**, 368-375.; H. Sun, S. Liu, W. Lin, K. Y. Zhang; W. Lv, X. Huang, F. Huo, H. Yang, G. Jenkins, Q. Zhao and W. Huang, *Nature Communications*, 2014, **5**, 3601.
- Y.Q. Sun, J. Liu, H. Zhang, Y. Huo, X. Lv, Y. Shi and W. Guo, *J. Am. Chem. Soc.*, 2014, **136**, 12520–12523; J. Liu, Y.Q. Sun, Y. Huo, H. Zhang, L. Wang, P. Zhang D. Song, Y. Shi and W. Guo, *J. Am. Chem. Soc.*, 2014, **136**, 574–577; B. Yang, J. Liu, H. Zheng and S. X. A. Zhang, *Chin. J. Chem.*, 2013, **31**, 1483-1487.
- G. He, D. Guo, C. He, X. Zhang, X. Zhao, and C. Duan, *Angew. Chem. Int. Ed.*, 2009, **48**, 6132–6135; Y. Yang, M. Lowry, C. Schowalter, S. Fakayode, J. Escobedo, X. Xu, H. Zhang, T. Jensen, F. Fronczek, I. Warner, and R. Strongin, *J. Am. Chem. Soc.*, 2006, **128**, 14081-14092.
- C. Yuan, S. Saito, C. Camacho, S. Irle, I. Hisaki and S. Yamaguchi. *J. Am. Chem. Soc.*, 2013, **135**, 8842–8845; H. Tong, Y. Hong, Y. Dong, Y. Ren, M. Haussler, J. Y. Lam, K. S. Wong, and B. Z. Tang, *J. Phys. Chem. B*, 2007, **111**, 2000-2007; Z. Zhang, Y. S. Wu, K. C. Tang, C. L. Chen, J.W. Ho, J. Su, H. Tian and P.T. Chou, *J. Am. Chem. Soc.*, 2015, **137**, 8509–8520; L. Wang, K. Wang, H. Zhang, C. Jiao, B. Zou, K. Ye and Y. Wang, *Chem. Commun.*, 2015, **51**, 7701–7704; Y. Dong, B. Xu, J. Zhang, X. Tan, L. Wang, J. Chen, H. Lv, S. Wen, B. Li, L. Ye, B. Zou and W. Tian, *Angew. Chem. Int. Ed.*, 2012, **51**, 10782–10785; X. Zhu, R. Liu, Y. Li. H. Huang, Q. Wang, D. Wang, X. Zhu, S. Liu and H. Zhu, *Chem. Commun.*, 2014, **50**, 12951–12954; Q. Qi, X. Fang, Y. Liu, P. Zhou, Y. Zhang, B. Yang, W. Tian and S. X. A. Zhang, *RSC Adv.*, 2013, **3**, 16986–16989.
- J. Cheng, D. Liu, L. Bao, K. Xu, Y. Yang and K. Han, *Chem. Asian J.*, 2014, **9**, 3215 – 3220; M. Santra, B. Roy, and K. H. Ahn, *Org. Lett.*, 2011, **13**, 3422-3425.
- R. Hu, S. Li, Y. Zeng, J. Chen, S. Wang, Y. Li and G. Yang, *Phys. Chem. Chem. Phys.*, 2011, **13**, 2044–2051.
- W. Lin, L. Yuan, Z. Cao, T. Feng and J. Z. Song, *Angew. Chem. Int. Ed.*, 2010, **49**, 375–379; N. Kumar, V. Bhalla and M. Kumar, *Analyst*, 2014, **139**, 543–558; L. Zhou, X. Zhang, Q. Wang, Y. Lv, G. Mao, A. Luo, Y. Wu, Y. Wu, J. Zhang and W. h. Tan, *J. Am. Chem. Soc.* 2014, **136**, 9838–9841.
- M. J. Frisch, G. W. Trucks, H. B. Schlegel, G. E. Scuseria, M. A. Robb, J. R. Cheeseman, G. Scalmani, V. Barone, B. Mennucci, G. A. Petersson, H. Nakatsuji, M. Caricato, X. Li, H. P. Hratchian, A. F. Izmaylov, J. Bloino, G. Zheng, J. L. Sonnenberg, M. Hada, M. Ehara, K. Toyota, R. Fukuda, J. Hasegawa, M. Ishida, T. Nakajima, Y. Honda, O. Kitao, H. Nakai, T. Vreven, J. Montgomery, J. A. , J. E. Peralta, F. Ogliaro, M. Bearpark, J. J. Heyd, E. Brothers, K. N. Kudin, V. N. Staroverov, R. Kobayashi, J. Normand, K. Raghavachari, A. Rendell, J. C. Burant, S. S. Iyengar, J. Tomasi, M. Cossi, N. Rega, J. M. Millam, M. Klene, J. E. Knox, J. B. Cross, V. Bakken, C. Adamo, J. Jaramillo, R. Gomperts, R. E. Stratmann, O. Yazyev, A. J. Austin, R. Cammi, C. Pomelli, J. W. Ochterski, R. L. Martin, K. Morokuma, V. G. Zakrzewski, G. A. Voth, P. Salvador, J. J. Dannenberg, S. Dapprich, A. D. Daniels, O. Farkas, J. B. Foresman, J. V. Ortiz, J. Cioslowski, and D. J. Fox, *Gaussian 09*, (Revision A. 02), Gaussian, Inc., Wallingford, CT 2009.
- Z. An, C. Zheng, Y. Tao, R. Chen, H. Shi, T. Chen, Z. Wang, H. Li, R. Deng, X. Liu and W. Huang, *Nature Materials*, **14**, 685–690.
- M. Cai, Z. Gao, X. Zhou, X. Wang, S.Chen, Y. Zhao, Y. Qian, N. Shi, B. Mi, L. Xie and W. Huang, *Phys. Chem. Chem. Phys.*, 2012, **14**, 5289–5296; Y. Qian, S. Li, G. Zhang, Q. Wang, S. Wang, H. Xu, C. Li, Y. Li, and G. Yang, *J. Phys. Chem. B*, 2007 **111**, 5861-5868.
- G. S. Jiao, L. H. Thoresen, and K. Burgess, *J. Am. Chem. Soc.* 2003, **125**, 14668-14669; X. Zhang, Y. Xiao, L. He, and Y. Zhang, *J. Org. Chem.* 2014, **79**, 6315–6320; Y. Ueno, J. Jose, A. Loudet, C. Perez-Bolivar, P. Anzenbacher, Jr. and K. Burgess, *J. Am. Chem. Soc.* 2011, **133**, 51–55.

An organic single-molecule RGB luminescence material with high quantum yields was realized by introducing ESIPT and TBET mechanism and combining an AIEE luminophore with a fluorescent switch.

